BASIC SCIENCE

Nanomedicine: Nanotechnology, Biology, and Medicine
13 (2017) 1853 – 1862

Original Article

nanomedjournal.com

Thermo-sensitive assembly of the biomaterial REP reduces hematoma volume following collagenase-induced intracerebral hemorrhage in rats

Joohyun Park[a,b], Jong Youl Kim[a], Seong-Kyoon Choi[d], Jae Young Kim[a], Jae Hwan Kim[c], Won Bae Jeon[d,*], Jong Eun Lee[a,b,**]

[a]*Department of Anatomy Yonsei University College of Medicine, Seoul, Republic of Korea*
[b]*BK21 Plus Project for Medical Science and Brain Research Institute, Yonsei University College of Medicine, Seoul, Republic of Korea*
[c]*Center for Neuroscience Imaging Research (CNIR), Institute for Basic Science (IBS), Suwon, Republic of Korea*
[d]*Laboratory of Biochemistry and Cellular Engineering, Daegu Gyeongbuk Institute of Science and Technology (DGIST), Daegu, Republic of Korea*

Received 4 August 2016; accepted 3 April 2017

Abstract

Intracerebral hemorrhage (ICH) frequently results in severe disabilities and high mortality. RGD-containing elastin-like polypeptide (REP), a modified elastin-like polypeptide (ELP), is a thermally responsive biopolymer. REP has high affinity for cells and is known to show non-immunotoxicity, -cytotoxicity, and -inflammatory responses. Here we found that administration of REP in the acute phase of the ICH rat model reduced the hematoma volume, decreased the number of activated microglia, attenuated the expression of von Willebrand Factor (vWF), and prevented the leakage of immunoglobulin G (IgG) into the cerebral parenchyma without any occlusion of intact microvessels. Therefore, the present data suggest that REP treatment could be a novel therapeutic strategy for attenuating the acute phase of ICH.

Key words: Intracerebral hemorrhage; Elastin-like polypeptide; Nanomaterial; RGD-containing elastin-like polypeptide

Intracerebral hemorrhage (ICH) is one of the most fatal diseases and it represents about 15% of all strokes worldwide.[1] When cerebral vessels are ruptured by a traumatic damage or an aneurysm, the parenchyma surrounding the injured vessels is aggravated by the high pressure induced by blood leakage, resulting in the damage of the cerebral tissue. The neurological dysfunction is directly caused by tissue destruction, increasing compression, and brain edema.[2] Approximately 75% of all patients with a spontaneous onset of ICH die or suffer from disabilities within a year, and mortality rates at 1 month account for 40% of all deaths.[1,3,4] Although many clinical trials related to ICH have been run, there is a lack of novel therapeutic strategies for treating ICH.

Elastin, an extracellular matrix constituent, provides elasticity and resilience that are necessary to sustain tissues construction such as skin and blood vessels.[5,6] Elastin-like polypeptide (ELP) is derived from human tropoelastin and composed of poly (Val-Pro-Gly-Xaa-Gly) pentapeptide, wherein Xaa can be any amino acid except proline.[6–9] ELP is non-cytotoxic, easily biodegradable, and can be used for several types such as hydrogel, microfiber, and cell sheet.[10–15]

The most remarkable characteristic of ELP is its thermo-sensitive responsiveness. At a specific temperature called transition temperature (T_t), ELP changes its own physical properties. Above T_t, ELP becomes insoluble and assumes an aggregated form. However, below T_t, ELP becomes soluble and

This research was supported by the Brain Research Program through the National Research Foundation of Korea (NRF) funded by the Ministry of Science, ICT & Future Planning to JEL (NRF-2016M3C7A1905098) and to WBJ (2014R1A2A2A01005619).

The authors have no conflict of interest to declare.

*Correspondence to: W. B. Jeon, Laboratory of Biochemistry and Cellular Engineering, Daegu Gyeongbuk Institute of Science and Technology (DGIST), Daegu 711-873, Republic of Korea.

**Correspondence to: J. E. Lee, Department of Anatomy, Brain Korea 21 Plus Project for Medical Science, Brain Research Institute, Yonsei University College of Medicine, Seoul 03722, South Korea.

E-mail addresses: wbjeon@dgist.ac.kr (W.B. Jeon), jelee@yuhs.ac, jelee@yumc.yonsei.ac.kr (J.E. Lee).

http://dx.doi.org/10.1016/j.nano.2017.04.001

it is found in a monomeric form.[6,16–18] The biocompatibility of ELP relies on its chemical similarity to human tropoelastin, (i.e. an elastin precursor) and it is therefore highly suitable for living cells. However, low cell adhesiveness of ELP and its lack of biological function limit its application to cell growth.[19] To circumvent these hurdles, the repetitive integrin-binding ArgGlyAsp (RGD) peptide containing ELP (V140) fusion protein, TGPG[VGRGD(VGVPG)6]20WPC, named REP, was developed.[7] REP is capable of promoting the adhesion and proliferation of neuronal cells on a poorly adherent organic scaffold.[20] In the present study, we hypothesize that REP scaffold plays a pivotal role in blocking a ruptured vessel and reducing the volume of hematoma. Therefore, we predict that an ICH-induced proinflammatory response, such as the activation of resident microglia changing to M1 phenotype, can be mitigated. In addition, damaged blood vessels may be repaired.[21] To verify our prediction, we measured the volume of the hematoma and we analyzed the inflammatory responses using immunohistochemistry. Here we show that REP administration reduces the volume of the hematoma, decreases the leakage of IgG to the brain parenchyma, attenuates the activation of microglia immune responses, and reduces the expression of von Willebrand factor (vWF) following ICH.

Methods

Animals

All animal care and surgical procedures were approved by the Institutional Animal Care and Use Committee (IACUC) of the Yonsei Laboratory Animal Research Center (YLARC).

Eight-week-old, male Sprague–Dawley (SD) rats (250-260 g) were purchased from Orient (Gyeonggi-Do, Korea) and were housed in a temperature- and humidity-controlled specific-pathogen free (SPF) zone under a 12-h light–dark cycle.

Intracerebral hemorrhage (ICH) model

All rats were anesthetized with an intraperitoneal (i.p.) injection of a mixture of zoletil (100 mg/kg, Virbac, USA) and xylazine (rompun, 10 mg/kg, Bayer, Germany). Body temperature of the rats was maintained at 36.5 °C-37.5 °C with heating pads and it was monitored with rectal probes. The rats were placed in a stereotactic apparatus, and a 30-gauge needle was implanted into the striatum (anterior: 0.2 mm, lateral: 3 mm, ventral: 6 mm). We then injected collagenase type VII (0.5 unit, 2 μL) for 10 min and the syringe was slowly (i.e. 10 min) retracted from the skull. After the surgical procedure, the holes were sealed with bone wax (Ethicon, USA).[22–24]

Preparation and characterization of REP and 5-carboxyfluorescein-labeled REP (FAM-REP)

The necessary procedures of REP synthesis have been previously reported.[7] Briefly, the ELP was expressed and purified in *Escherichia coli* BLR (DE3) by inverse transition cycling. Contents of repetitive integrin-binding AspGlyAsp (RGD) peptides and VG (VGVPG) domains were computed using Compute pI/MW. The fusion protein (REP), which is purified ELP (V140)-RGD peptide, was dissolved in cold PBS (pH 7.2, Gibco, USA). To characterize the thermal transition, the changes in temperature and absorbance at 350 nm were monitored with Cary Win-UV software. The T_t was defined as the temperature at which 50% of the maximal turbidity was observed.

The preparation and characterization related with FAM-REP have been previously described.[10] In brief, to conjugate 5-carboxyfluorescein (FAM) to the N-terminus of REP, 5-carboxyfluorescein N-succinimidyl ester (5.0 μmol) in dimethyl sulfoxide (580 μL) was added to REP (0.97 μmol) in PBS (20 mL). The mixture was reacted at room temperature for 3 h to generate FAM-labeled REP. FAM-REP was purified by performing 3 cycles of repeated inverse phase transition at 4 °C for cooling and 45 °C for heating. The degree of FAM labeling was determined according to the protocol in the AnaTag™ protein labeling kit (AnaSpec). The T_t is the temperature at which solubilized REP forms highly hydrated hydrogel-like aggregates. The inverse T_t of REP is determined by REP's concentration.

Jeon and colleagues reported that the transition curves of three REP solutions were characterized in a dose-dependent manner (20, 50, and 100 μM). When the temperature of the solution was increased from 15 °C to 35 °C, all three solutions exhibited an elevation in absorbance due to REP aggregation. T_t values were determined to be 29.7, 25.9, and 25.3 °C for 20, 50, and 100 μM REP, respectively. Because these T_t values were lower than the mouse body temperature, the REP solutions spontaneously self-assembled into gel-like aggregates after topical loading into the injured space.[10]

Drug treatment

All rats were re-anesthetized 3 h after ICH and underwent an incision on the neck along the midline. The right external carotid artery (rECA) and the right common carotid artery (rCCA) permanently tied with 4-0 silk sutures. After ligation of the arteries, 100 μL of cold PBS (ICH + PBS group, n = 30) or an equal volume of REP dissolved in cold PBS (ICH + REP group, 100 μM/100 μL, n = 40) were administered with an insulin syringe through the right internal carotid artery (rICA).

Measurement of the hematoma volume

For the histological examination and the quantification of the hematoma volume, rats were sacrificed 6, 24, or 48 h after ICH. Rats were deeply anesthetized with an intraperitoneal (i.p.) injection of a mixture of zoletil (100 mg/kg) and xylazine (rompun, 10 mg/kg), transcardially perfused with PBS and 4% paraformaldehyde in 0.1 mol/L phosphate-buffered saline. After the cardiac perfusion, the brain was removed and sliced into 2 mm thick coronal sections. The percentage of hematoma volume [(hematoma volume / hemispheric brain volume) × 100] was measured using Image J.[25]

Immunohistochemistry

Fixed brain tissue was washed with PBS for 6 h and placed in cryoprotectant (30% sucrose) for 3 days. The tissue was embedded in OCT compound and transferred to −80 °C. Frozen sections (n = 6, per group) were sliced into 10 μm thick section and air dried at room temperature. For the immunofluorescence

analysis, the sections (n = 5, per group) were fixed in cold methanol for 15 min at −20 °C. After fixation, the sections were blocked with donkey serum (1:10) for 1 h at room temperature to avoid non-specific binding. The following primary antibodies were used overnight at 4 °C: polyclonal anti-rat IgG (1:50, Invitrogen, Carlsbad, CA, USA) for the detection of IgG leakage in the parenchyma, anti-Iba1 (1:200, Abcam, Cambridge, UK) for detecting activated microglia, anti-PECAM (1:50, Santa Cruz, Dallas, Texas, USA) for labeling endothelial cells (ECs), and anti-von Willebrand Factor (vWF, 1:200, Abcam, Cambridge, UK) for ECs. The slides were washed in PBS three times and incubated with the appropriate secondary antibodies conjugated either with rhodamine (1:200, Millipore) or fluorescein isothiocyanate (FITC, 1:200, Millipore) for 1 h at room temperature in a dark chamber. The slides were stained with 4,6-diamidino-2-phenylindole (DAPI, Vector, Burlingame, USA) to counter-stain the nuclei and mounted with cover slip. All images were acquired with a confocal microscope (LSM700, Carl Zeiss, Thornwood, NY, USA).

2,3,5-triphenyl-2H-tetrazolium chloride (TTC) staining

Rats were deeply anesthetized and injected with REP through the intra-arterial route; namely, the right internal carotid artery (rICA). Rats were euthanized 3, 6, and 24 h after the administration of REP. The brains were removed and sliced into 2 mm-thick after cardiac perfusion with PBS, and the sections were transferred to a 2% TTC (Santa Cruz, Dallas, Texas, USA) solution at 37 °C for 20 min.

Cell adhesion assay

A 96-well plate was coated with REP at different concentrations (0, 0.2, 0.6, 1.0 μM) and then incubated at 4 °C. After 12 h of coating, excess REP was removed and wells were washed two times with 200 μL PBS. Brain endothelial cells (b.End3 cell, 2×10^5 in 200 μL DMEM) were seeded in each well and incubated for 1 h. After removing the culture medium, the wells were washed quickly two times with 200 μL of cold PBS to eliminate unattached cells. Subsequently, wells were treated with 200 μL of ice-cold 100% methanol at 25 °C for 10 min to fix the cells. After fixation, the wells were rinsed three times with PBS and 100 μL of crystal violet solution was added (0.5% w/v crystal violet in 20% ethanol) and incubated for 20 min at 25 °C. After incubation, the wells were washed three times with PBS to remove excess crystal violet. Stained cells were recovered by adding 200 μL of 100% methanol to each well, and gently shaking the plate for 10 min at 25 °C. Finally, extracted crystal violet was measured at 590 nm by using a microplate reader (Multiskan, Thermoscienfic, USA).

Statistical analysis

All statistical analyses were performed using SPSS 18.0 software (IBM Corp., Armonk, NY, USA). Data were presented as mean ± standard error of the mean (S.E.M). A one-way repeated measures ANOVA was used to compare the differences between experimental groups. The Tukey's post hoc multiple comparison tests was used for further group comparisons. Differences were considered statistically significant at $p < 0.05$ (*$p < 0.05$, **$p < 0.01$, *** $p < 0.001$).

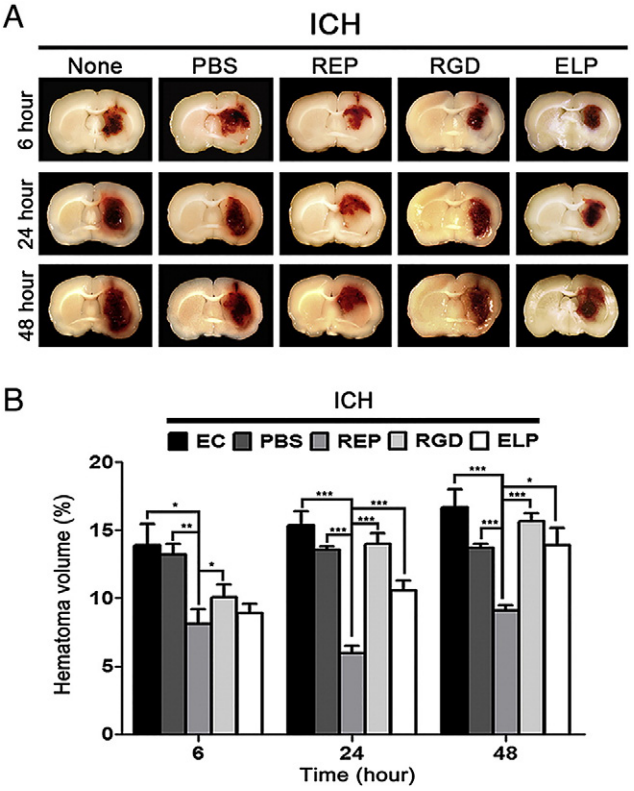

Figure 1. Time-dependent changes of the percentage of the hematoma volume following ICH. **(A)** Time-dependent changes of hematoma volume. **(B)** The volume of hematoma significantly reduced in ICH + REP groups compared to ICH-only, ICH + PBS, ICH + RGD, and ICH + ELP (V140) groups (n = 7-8/group, *$p < 0.05$, **$p < 0.01$, ***$p < 0.001$, Tukey's post-hoc test).

Results

Analysis of the hematoma volume following ICH

To evaluate the volume of the hematoma, different groups of rats were sacrificed either 6, 24 or 48 h after the collagenase-induced intracerebral hemorrhage (Figure 1, *A*). The volume of the hematoma at the 6 h time point was significantly reduced in the ICH + REP group (8.1%) as compared to ICH-only (13.9%), ICH + PBS (13.2%), ICH + RGD (10.1%), and ICH + ELP (V140) (9.3%) groups. The percentage number represents the hematoma volume [(hematoma volume / hemispheric brain volume) × 100].

However, no statistical difference was found between ICH + ELP (V140) group and ICH + REP group at 6 h. Moreover, hematoma volume of the ICH + REP group (6.0%) considerably reduced, compared to ICH-only (15.4%), ICH + PBS (13.6%), ICH + RGD (14%), and ICH + ELP (V140) (10.6%) groups 24 h post-ICH. In addition, the level of hematoma gradually decreased in the ICH + REP group (9.1%) when compared to ICH-only (16.7%), ICH + PBS (13.7%), ICH + RGD (15.6%), and ICH + ELP (V140) (13.9%) groups 48 h post-ICH. (Figure 1, *B*). Taken together, the REP treatment reduces the hematoma volume statistically significantly after collagenase-induced ICH injury.

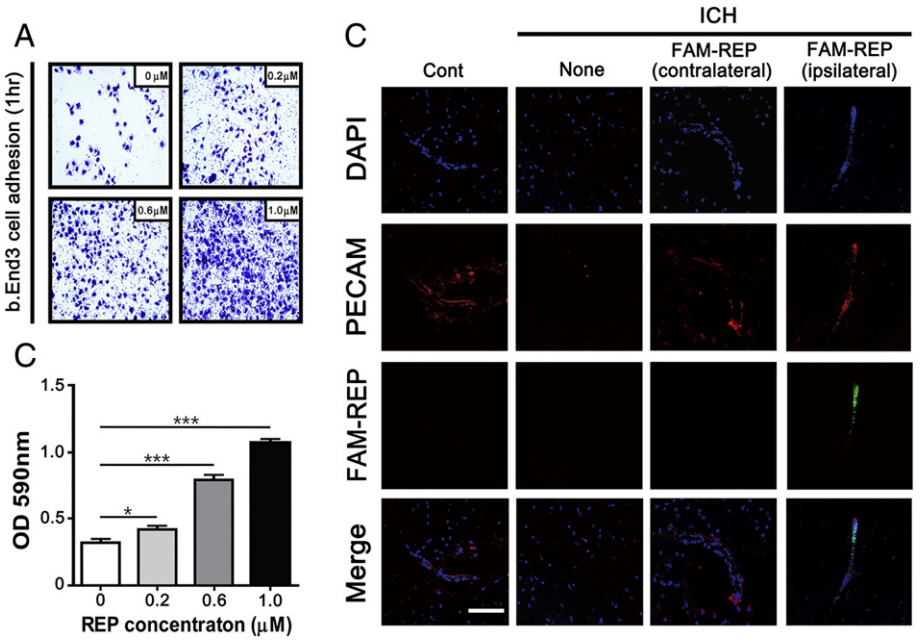

Figure 2. Cell adhesion assay and observation of specifically targeted FAM-labeled REP following intracerebral hemorrhage (ICH). REP is located at the target lesion at the ipsilateral site and enhances cell adhesion after injection. **(A)** Crystal violet-stained cells attached to plates coated with REP at different concentrations. Images were taken 1 h after adhesion time. **(B)** Comparison of REP dose-dependent cell adhesion. **(C)** Fluorescence-tagged REP was specifically observed in the ipsilateral site of the ICH + FAM-REP group (green). No fluorescence was observed in the ICH-only group (negative control) and the contralateral site of the ICH + FAM-REP group. PECAM was used as an endothelial cell marker. Cell nuclei were stained with DAPI. (*$p < 0.05$, **$p < 0.01$, ***$p < 0.001$, scale bar = 100 μm, Dunnett's multiple comparison test).

Improved brain endothelial cell (b.End3 cell) adhesion and REP location

During bleeding after traumatic injury, endothelial cells lining the lumen of blood vessels are exposed. We hypothesized that REP injected via rICA would adhere to endothelial cells. Thus, the exposed lesion would be covered and filled with REP. To investigate whether REP induces the adhesion of b.End3 cells, a cell adhesion assay using crystal violet was performed (Figure 2, *A* and *B*). The b.End3 cells were seeded onto plates dose-dependently coated with REP (0.2, 0.6, 1 μM). After 1 h incubation, the percentage of attached cells in wells containing REP was approximately 141%, 246%, and 334% relative to control (0 μM, PBS). The b.End3 cells cultured on a 1 μM REP-coated plate were approximately 2.3 times higher than on control plates. Next, to confirm that REP administered via arterial injection reached the target lesion, FAM-labeled REP was injected into the rICA after ICH and the brain slices were stained above T_t (25 °C) and inspected using a confocal microscope. Because the major feature of REP is its ability to undergo thermal-induced phase transitions, minor modifications were made to the following procedures. We detected FAM-tagged REP on the ipsilateral, but not on the contralateral site of brains taken from the FAM-labeled REP group. FAM-like fluorescence (i.e. a pseudo-positive signal) was not observed in the ICH-only group. FAM-labeled REP changed its physical property from liquid to gel-like aggregates upon in vivo administration.[10] Gel-like FAM-labeled REP could adhere to the perihematomal cells and specifically blocked ruptured vessels (Figure 2, *C*). Therefore, our findings suggest that REP promotes endothelial cell adhesion and is specifically located at the lesion site. These data support our TTC staining results indicating that REP treatment does not cause infarction of healthy microvessels.

Relationship between obstruction of intact microvessels and administration of REP

The 2,3,5-triphenyl-2H-tetrazolium chloride (TTC) staining is generally used to assess cellular respiration so that metabolically active and inactive tissues can be distinguished; active tissue is stained with a deep red color, while the inactive tissue is white. The TTC staining was used to confirm that the injected REP aggregating into the right internal carotid artery (rICA) specifically targets the lesion without occluding any other intact microvessels. Three control rats were sacrificed at 3, 6 or 24 h after administration of REP without ICH (Cont + REP). No ischemic infarction was observed upon REP administration in groups (Figure 3). These results indicate that the thermo-sensitive and reversible REP is biologically stable in vivo by maintaining microvessels intact without infarction even upon environmental changes.

Amount of the perivascular blood component IgG protein leakage into parenchyma lesion after ICH

Based on the in vivo results showing the decreased hematoma volume following the REP administration, we performed immunohistochemistry to confirm the extent of IgG, a

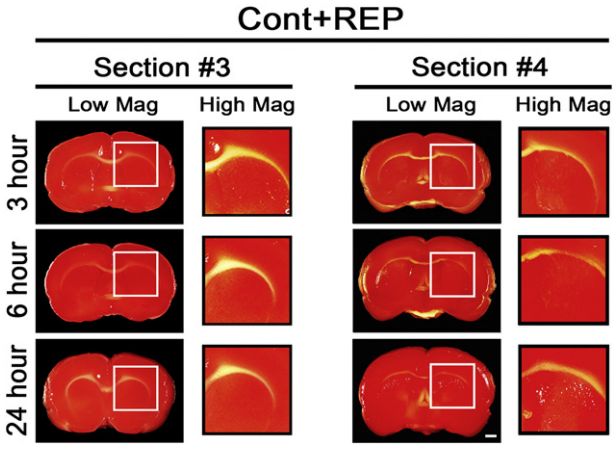

Figure 3. 2,3,5-triphenyl-2H-tetrazolium chloride(TTC) staining. TTC staining was performed 3, 6 and 24 h after administration of REP in normal control (Cont). No ischemic infarction was found in Cont + REP groups. (low magnification =10×, high magnification =20×, scale bar =2 mm).

component of blood plasma, vascular leakage throughout the ruptured cerebral vessels to the parenchyma lesion in the striatum. In ICH-only and ICH + PBS groups, IgG was highly expressed compared to ICH + REP groups at all time points (Figure 4, *A-C*); the relative percentage of IgG-positive area in ICH + REP group (10.2%) was approximately less than half, compared to ICH-only (20.7%) and ICH + PBS treated (20.3%) groups at 6 h. Furthermore, the data showed that the extent of IgG leakage in ICH + REP group (8.3%) was significantly reduced compared with ICH-only (29.1%) and ICH + PBS (25.0%) groups at 24 h post-ICH. Additionally, the relative percentages of expression of IgG-positive area in ICH-only, ICH + PBS and ICH + REP groups were approximately 23.5%, 20.5%, and 9.0%, respectively. These values were ~2 times lower than those of ICH-only and ICH + PBS groups, at 48 h post-ICH (Figure 4, *D*). These data indicate that REP blocks the leakage of blood components from ruptured vessels to brain parenchyma following ICH.

Alteration of the cerebrovascular integrity by the administration of REP after ICH

To assess the cerebrovascular integrity, we performed an immunohistochemistry using the anti-von Willebrand Factor (vWF) antibody for detecting the damaged brain vessels and the anti-platelet-endothelial cell adhesion molecule (PECAM) antibody as a marker for blood vessels. vWF, a multimeric glycoprotein, plays a crucial role in the coagulation system and it is composed of multiple subunits produced by endothelial cells and megakaryocytes. In addition, molecules of vWF are stored in endothelial cells and in alpha-granules of platelets. vWF is necessary for platelets to adhere to exposed subendothelial collagen in arterioles. When bleeding caused by traumatic injury, vWF provides receptor sites for platelet and collagen. The primary receptor sites replace exposed subendothelial collagen known as innermost vascular lining site, and bind a surface receptor of platelet and glycoprotein Ib/IX/V.[26,27] Then, activated platelets adhere by binding vWF. The larger vWF multimers form a fibrillar carpet on which the platelets assemble. The expression of vWF significantly increased in ICH-only and ICH + PBS groups compared to Cont and ICH + REP groups 6 h after ICH (Figure 5, *A* and *D*). Moreover, vWF was highly expressed in ICH-only and ICH + PBS groups compared to Cont and ICH + REP groups 24 h after ICH (Figure 5, *B* and *D*).

Furthermore, vWF expression was substantially augmented in ICH-only and ICH + PBS groups compared with Cont and ICH + REP groups 48 h after, respectively (Figure 5, *C* and *D*). These data indicate that REP enhances vessel integrity and reduces the overexpression of vWF by replacing the role of vWF filling the exposed subendothelial collagen site after ICH injury.

Microglial activation after ICH injury

Resident microglia interacting with neurons in the central nervous system (CNS) exerts an important function similar to macrophages fighting against viral, bacterial, and fungal infections in periphery. The resident microglia changes to activated forms that act as macrophages when they are stimulated by molecular cues. Interestingly, microglia activation has been considered detrimental for the treatment of many neurological diseases.[28–30] To detect the activated microglia following ICH, we used the anti-ionized calcium binding adapter molecule 1 (Iba1) antibody which specifically detects activated microglia.[31]

To test whether the REP treatment on the traumatic brain injury causes a negative effect like an immune response, we performed an immunohistochemistry specific for active microglia. We found that Iba1-positive cells were gradually increased in all groups. The relative number of Iba1-positive cells, however, significantly declined in ICH + REP groups compared to the other groups. At 6 h, the percentage of Iba1-positive microglia in the ICH-only, ICH + PBS and ICH + REP groups were 24.6%, 30.0%, and 9.3%, respectively (Figure 6, *A* and *D*). Moreover, the number of Iba1-positive cells in the ICH + REP group was significantly lower than the number of cells observed in the ICH-only and ICH + PBS groups 24 h post-ICH. The percentages of Iba1-positive cells were 11%, 36.3%, and 37.2% in the ICH + REP, ICH-only and ICH + PBS groups, respectively (Figure 3, *B* and *D*). Also, more Iba1-positive cells were detected in both ICH-only (47.9%) and ICH + PBS (37.8%) than in ICH + REP group (17.6%) 48 h post-ICH (Figure 6, *C* and *D*).

These data suggest that the administration of REP ameliorates the activation of microglia that occur as an immune response associated with the detrimental roles played by the post-ICH activated microglia.

Discussion

In the present study, the administration of REP reduced the hematoma volume, prevented the leaking of the blood component into the cerebroparenchyma, and attenuated the migration of activated microglia to the perihematoma area. In addition, vWF expression levels in the ICH + REP group were significantly decreased compared to the other groups. These results were related to the reduction of the ICH injury, including the inflammatory responses. Previous findings showed that biosynthesized extracellular matrix (ECM) obtained from animal tissues have biological issues such as low adhesion, migration,

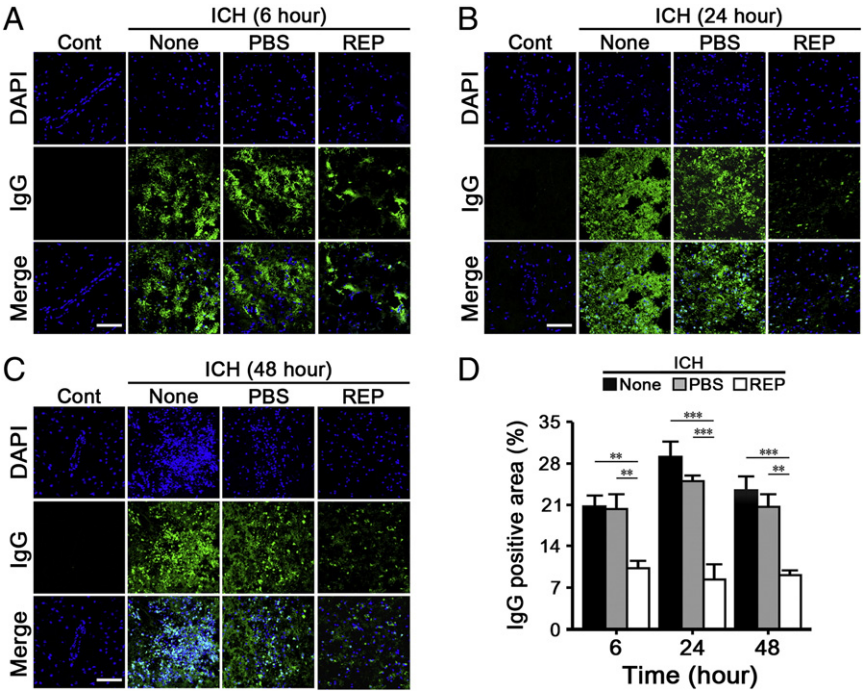

Figure 4. Percentage of positive-IgG area of the parenchyma lesion. **(A-C)** Immunohistochemistry showing the positive area of IgG in the brain parenchyma lesion. **(D)** At all time points, IgG expression is significantly reduced in ICH + REP group relative to ICH-only and ICH + PBS groups. (n = 5/group, $*p < 0.05$, $**p < 0.01$, $***p < 0.001$, scale bar = 100 μm, Tukey's post-hoc test.)

proliferation, and differentiation of either implanted or adjacent cells. Moreover, immunological response issues such as the cytotoxicity had not been entirely resolved.[7,32,33] Genetically engineered biopolymers such as the ELP modeled by human tropoelastin are considered novel biomaterials for the biomedical fields. ELP has some promising properties for biological applications: biocompatibility, biodegradability, and non-immunogenicity. Above all, ELP reacts to thermal changes through a soluble-insoluble phase transition. As a consequence, ELP becomes a gel type above the T_t, and transition to a sol type below T_t.[6,16–18,34–36] Several researchers have exploited this ELP feature for drug and gene delivery in oncology.[37–43] Although an ELP with low immunotoxicity and cytotoxicity is highly compatible with living cells and can be controlled at the gene level, there are limitations in the ability of this compound to interact with cells. Indeed, ELP shows reduced adhesive properties and limited capability to sustain cell growth.[19,36] In this study, administration of ELP (V140) alone after ICH slightly but not significantly reduced the volume of hematoma in time-dependent manners. Particularly, the effect of ELP to reduce hematoma volume could hardly be observed at 48 h after injury.

A newly biosynthesized extracellular matrix, named REP, TGPG[VGRGD(VGVPG)$_6$]$_{20}$WPC fused with cell-adhesive integrin Arg-Gly-Asp (RGD) ligands and elastin-derived VGVPG pentapeptides has been reported recently.[7,20,44] A previous study showed that both the adhesion and proliferation of neuronal progenitor cells (NPCs) were considerably up-regulated by REP on a poorly adhesive organic scaffold.[20] To improve the effect of ELP on ICH injury, ELP (V140)-based recombinant biomaterial REP was used in the present study and we investigated the effects of ELP (V140)-based recombinant biomaterial REP after ICH. REP administration significantly reduced the hematoma volume by 9.1%, compared to the results in ICH-only (16.7%), ICH + PBS (13.7%), ICH + RGD (15.6%), and ICH + ELP (V140, 13.9%) groups at the 48 h time point after ICH injury. These findings may suggest that REP treatment effectively reduces the hematoma volume after collagenase-induced ICH injury. In addition, the amount of IgG leakage following ICH was significantly decreased in the ICH + REP group compared to ICH-only and ICH + PBS groups. These results indicate that the injected thermo-sensitive and solubilized REP may form self-assembled coacervates above T_t and relocate to the hemorrhagic lesion, thereby covering the ruptured cerebral vessels.

Moreover, the number of activated microglia within parenchyma was reduced in the ICH + REP group compared to ICH-only and ICH + PBS groups.

The predominantly resident CNS macrophages, named microglia, are known as immune cells related to the inflammatory response. These cells transition to the activated form upon the invasion of microbes or other molecular cues. Activated microglia move to the hemorrhagic area by chemotaxis to remove blood components and other debris.[44–48] Therefore, our findings indicate that REP induces hemostasis and prevents the pressure-induced damage of peri-hematomal tissues caused by blood components leaking from the injured vessels. Consequently, the inflammatory response (i.e. the recruitment of macrophages to the hemorrhagic lesion) is reduced.

Moreover, self-assembled REP injected into the brain did not block any intact cerebral vessels in normal controls. Insufficient

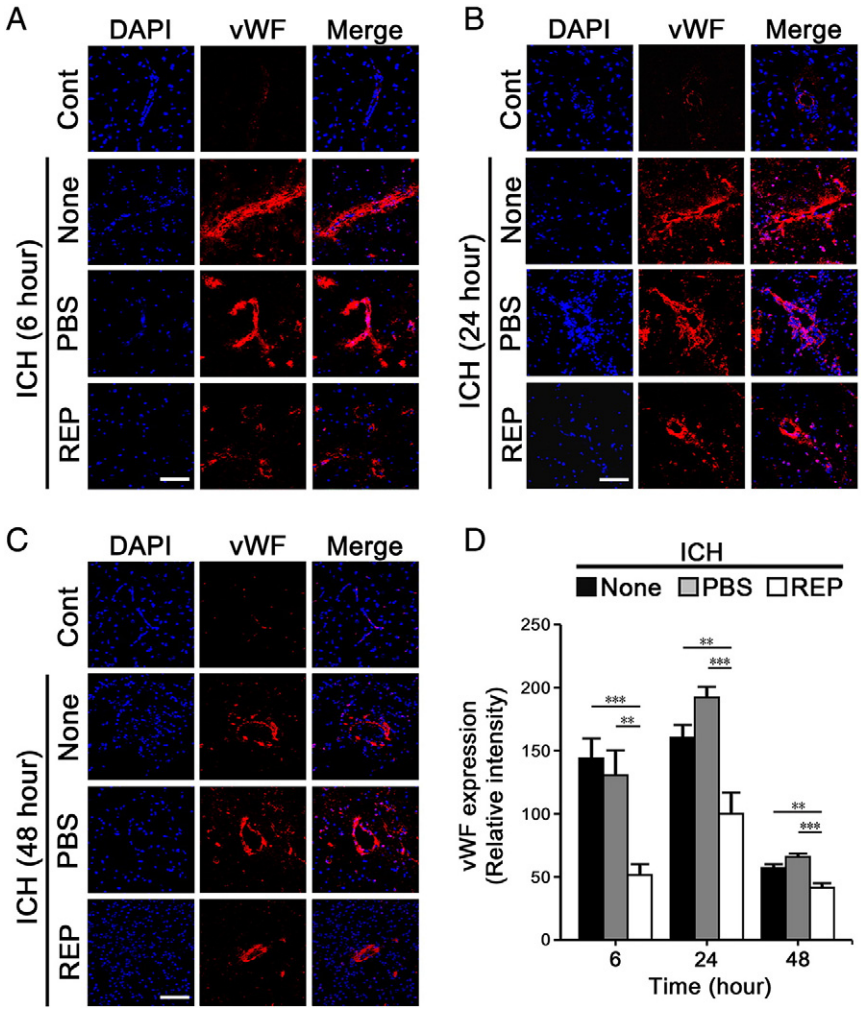

Figure 5. Immunohistochemistry staining showing the time-dependent expression of vWF following ICH. **(A-C)** Immunohistochemistry for vWF. The expression of vWF groups considerably reduced in ICH + REP relative to ICH-only and ICH + PBS groups at all time points. **(D)** vWF expression significantly decreased in ICH + REP groups relative to ICH-only and ICH + PBS groups (n = 6/group, *$p < 0.05$, **$p < 0.01$, ***$p < 0.001$, scale bar = 100 μm, Tukey's post-hoc test).

blood supply, or occlusion of cerebral vessels, induces cerebral ischemia. The result of the TTC staining indicates that REP injected into the rICA, became a self-assembling gel type above the T_t. However, it did not induce the infarction. However, further studies on the concentration and amount of REP inducing cerebral ischemia are required.

As mentioned above, vWF, a 600,000-D to 20,000,000-D glycoprotein secreted by endothelial cells, is an essential cofactor associated with the coagulation pathway and plays a crucial role in promoting the adhesion of platelets to the subendothelial collagen.[49] In the process of coagulation, vWF functions as a carpet between the exposed endothelial cells and activated platelets. In addition, vWF, which has an RGD sequence, binds platelet binding site. Indeed, it has been reported that endothelial cells are activated and the serum level of vWF is increased upon traumatic brain injury.[27,50,51] In this study, we predicted that REP injected into the rICA may play an important role as a carpet, in analogy with the role played by vWF in the damaged cerebrovessels, thereby attenuating the bleeding in the early stage of ICH, as well as reducing the expression of vWF. Consistent with our prediction, the present findings indicate that the expression of vWF following ICH was significantly reduced in the REP-treated group as compared to ICH-only and ICH + PBS groups. However, whether REP interacts with platelets in the early phase of hemostatsis following ICH is still unknown and needs further studies.

Furthermore, FAM-labeled REP was specifically located in the perihematomal parenchyma of the ipsilateral side. A hyperthermic reaction is spontaneously induced in response to inflammation, which can be caused by microbial infection as well as ischemic or hemorrhagic stroke.[52–54] We demonstrated that injected FAM-labeled REP molecules primarily accumulated in the ruptured vessels of the ipsilateral, but not the contralateral site. However, the cohesiveness and half-life of REP according to arterial blood flow must be determined in future studies. Moreover, the efficiency and the effects of REP related to the delivery routes (e.g. local injection, intraperitoneal, intravascular, and oral administration) should be tested in future

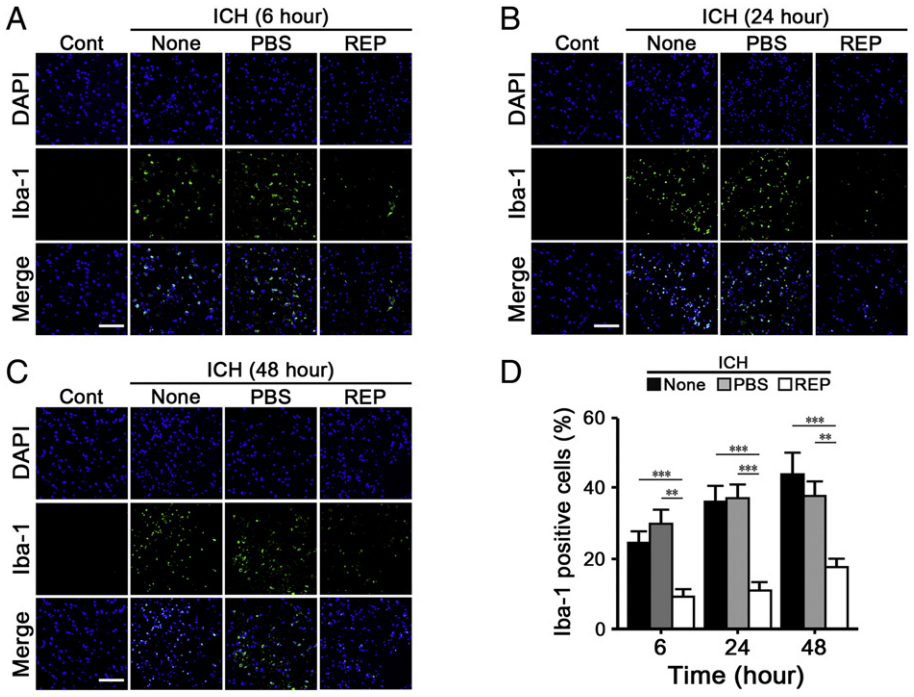

Figure 6. Percentage of Iba1-positive microglia in parenchyma lesion after ICH. **(A-C)** Immunohistochemistry showing the Iba1-positive microglia in the parenchyma lesion. **(D)** Activated microglia (% Iba1-positive cell, green) were decreased in ICH + REP groups relative to ICH-only and ICH + PBS groups at all time points. (n = 5/group, *$p < 0.05$, **$p < 0.01$, ***$p < 0.001$, scale bar = 100 μm, Tukey's post-hoc test.)

research. Additionally, contrary to our prediction that REP may specifically fill the ruptured part of vessels following ICH, transformed FAM-labeled REP in vivo was found to be covering cells located in perihematomal lesion. We speculated that this phenomenon was caused by the adhesiveness of REP. Finally, we found that REP improved endothelial cell attachment through cell adhesion assay. These data support our hypothesis, however, further studies are needed.

Recently, Jeon and colleagues revealed that infilling wounds with REP aggregates promotes host cell migration from the wound margins while enhancing the survival of engrafted adipose stem cell (ASC) through cell attachment. To better understand the mechanisms underlying the effects of REP, Jeon and colleagues measured the activation statuses of Fak, Src, Erk, and Akt signaling kinases, i.e. kinases that play important roles in cell adhesion, migration, and survival. Indeed, this mechanistic investigation suggested that the effects of REP are mediated through the activated Fak/Src signaling and the upregulation of Mek/Erk and PI3K/Akt survival pathways.[10] Therefore, we speculate that REP may exert its positive effects through the activation of the same pathway. However, the exact role played by REP in alleviating the brain damage needs further studies.

In conclusion, here we have shown that the administration of biosynthesized RGD motif based-REP through the rICA following ICH specifically covers the ruptured cerebral vessels. This positive action reduces the hematoma volume, prevents excessive leakage of blood components from vessels, attenuates the activation of microglia, and decreases the expression of vWF. Although the present investigation of REP effects are limited to the narrow time-window of the acute phase of the rat model of ICH, REP is a potential therapeutic agent for treating the acute phase IHC due to its non-immunogenicity, biocompatibility, biodegradability, and the several positive effects described in the present paper.

Acknowledgements

The authors would like to thank Dr. Young-Min Hyun and Dr. Daewon Moon for their critical suggestions, discussion, and comments during the preparation of this paper.

References

1. Brouwers HB, Chang Y, Falcone GJ, Cai X, Ayres AM, Battey TW, et al. Predicting hematoma expansion after primary intracerebral hemorrhage. *JAMA Neurol* 2014;**71**:158-164.
2. Lee JC, Cho GS, Choi BO, Kim HC, Kim YS, Kim WK. Intracerebral hemorrhage-induced brain injury is aggravated in senescence-accelerated prone mice. *Stroke* 2006;**37**:216-222.
3. Qureshi AI, Mendelow AD, Hanley DF. Intracerebral haemorrhage. *Lancet* 2009;**373**:1632-1644.
4. van Asch CJ, Luitse MJ, Rinkel GJ, van der Tweel I, Algra A, Klijn CJ. Incidence, case fatality, and functional outcome of intracerebral haemorrhage over time, according to age, sex, and ethnic origin: a systematic review and meta-analysis. *Lancet Neurol* 2010;**9**:167-176.
5. Floss DM, Schallau K, Rose-John S, Conrad U, Scheller J. Elastin-like polypeptides revolutionize recombinant protein expression and their biomedical application. *Trends Biotechnol* 2010;**28**:37-45.
6. Ryu JS, Raucher D. Elastin-like polypeptide for improved drug delivery for anticancer therapy: preclinical studies and future applications. *Expert Opin Drug Deliv* 2014:1-15.
7. Jeon WB, Park BH, Wei J, Park RW. Stimulation of fibroblasts and neuroblasts on a biomimetic extracellular matrix consisting of tandem

repeats of the elastic VGVPG domain and RGD motif. *J Biomed Mater Res A* 2011;**97**:152-157.
8. McDaniel JR, Callahan DJ, Chilkoti A. Drug delivery to solid tumors by elastin-like polypeptides. *Adv Drug Deliv Rev* 2010;**62**:1456-1467.
9. Ryu JS, Kuna M, Raucher D. Penetrating the cell membrane, thermal targeting and novel anticancer drugs: the development of thermally targeted, elastin-like polypeptide cancer therapeutics. *Ther Deliv* 2014;**5**:429-445.
10. Choi SK, Park JK, Kim JH, Lee KM, Kim E, Jeong KS, et al. Integrin-binding elastin-like polypeptide as an in situ gelling delivery matrix enhances the therapeutic efficacy of adipose stem cells in healing full-thickness cutaneous wounds. *J Control Release* 2016;**237**:89-100.
11. Betre H, Ong SR, Guilak F, Chilkoti A, Fermor B, Setton LA. Chondrocytic differentiation of human adipose-derived adult stem cells in elastin-like polypeptide. *Biomaterials* 2006;**27**:91-99.
12. Caves JM, Kumar VA, Martinez AW, Kim J, Ripberger CM, Haller CA, et al. The use of microfiber composites of elastin-like protein matrix reinforced with synthetic collagen in the design of vascular grafts. *Biomaterials* 2010;**31**:7175-7182.
13. Zhang H, Iwama M, Akaike T, Urry DW, Pattanaik A, Parker TM, et al. Human amniotic cell sheet harvest using a novel temperature-responsive culture surface coated with protein-based polymer. *Tissue Eng* 2006;**12**:391-401.
14. Lampe KJ, Antaris AL, Heilshorn SC. Design of three-dimensional engineered protein hydrogels for tailored control of neurite growth. *Acta Biomater* 2013;**9**:5590-5599.
15. Rincon AC, Molina-Martinez IT, de Las Heras B, Alonso M, Bailez C, Rodriguez-Cabello JC, et al. Biocompatibility of elastin-like polymer poly(VPAVG) microparticles: in vitro and in vivo studies. *J Biomed Mater Res A* 2006;**78**:343-351.
16. Reguera J, Urry DW, Parker TM, McPherson DT, Rodriguez-Cabello JC. Effect of NaCl on the exothermic and endothermic components of the inverse temperature transition of a model elastin-like polymer. *Biomacromolecules* 2007;**8**:354-358.
17. Reiersen H, Clarke AR, Rees AR. Short elastin-like peptides exhibit the same temperature-induced structural transitions as elastin polymers: implications for protein engineering. *J Mol Biol* 1998;**283**:255-264.
18. Urry DW, Gowda DC, Parker TM, Luan CH, Reid MC, Harris CM, et al. Hydrophobicity scale for proteins based on inverse temperature transitions. *Biopolymers* 1992;**32**:1243-1250.
19. Nicol A, Gowda DC, Parker TM, Urry DW. Elastomeric polytetrapeptide matrices: hydrophobicity dependence of cell attachment from adhesive (GGIP)n to nonadhesive (GGAP)n even in serum. *J Biomed Mater Res* 1993;**27**:801-810.
20. Choi SK, Park JK, Lee KM, Lee SK, Jeon WB. Improved neural progenitor cell proliferation and differentiation on poly(lactide-co-glycolide) scaffolds coated with elastin-like polypeptide. *J Biomed Mater Res B Appl Biomater* 2013;**101**:1329-1339.
21. Wu J, Yang S, Xi G, Song S, Fu G, Keep RF, et al. Microglial activation and brain injury after intracerebral hemorrhage. *Acta Neurochir Suppl* 2008;**105**:59-65.
22. Altumbabic M, Peeling J, Del Bigio MR. Intracerebral hemorrhage in the rat: effects of hematoma aspiration. *Stroke* 1998;**29**:1917-1922 [discussion 22-3].
23. Rosenberg GA, Mun-Bryce S, Wesley M, Kornfeld M. Collagenase-induced intracerebral hemorrhage in rats. *Stroke* 1990;**21**:801-807.
24. Tang T, Liu XJ, Zhang ZQ, Zhou HJ, Luo JK, Huang JF, et al. Cerebral angiogenesis after collagenase-induced intracerebral hemorrhage in rats. *Brain Res* 2007;**1175**:134-142.
25. Schneider CA, Rasband WS, Eliceiri KW. NIH image to ImageJ: 25 years of image analysis. *Nat Methods* 2012;**9**:671-675.
26. De Oliveira CO, Reimer AG, Da Rocha AB, Grivicich I, Schneider RF, Roisenberg I, et al. Plasma von Willebrand factor levels correlate with clinical outcome of severe traumatic brain injury. *J Neurotrauma* 2007;**24**:1331-1338.
27. Ruggeri ZM, Ware J. Von Willebrand factor. *FASEB J* 1993;**7**:308-316.
28. Banati RB, Gehrmann J, Schubert P, Kreutzberg GW. Cytotoxicity of microglia. *Glia* 1993;**7**:111-118.
29. Banati RB, Kreutzberg GW. Flow cytometry: measurement of proteolytic and cytotoxic activity of microglia. *Clin Neuropathol* 1993;**12**:285-288.
30. Kreutzberg GW. Microglia: a sensor for pathological events in the CNS. *Trends Neurosci* 1996;**19**:312-318.
31. Patro N, Nagayach A, Patro IK. Iba1 expressing microglia in the dorsal root ganglia become activated following peripheral nerve injury in rats. *Indian J Exp Biol* 2010;**48**:110-116.
32. Badylak SF, Gilbert TW. Immune response to biologic scaffold materials. *Semin Immunol* 2008;**20**:109-116.
33. Plow EF, Haas TA, Zhang L, Loftus J, Smith JW. Ligand binding to integrins. *J Biol Chem* 2000;**275**:21785-21788.
34. Rodriguez-Cabello JC, Pierna M, Fernandez-Colino A, Garcia-Arevalo C, Arias FJ. Recombinamers: combining molecular complexity with diverse bioactivities for advanced biomedical and biotechnological applications. *Adv Biochem Eng Biotechnol* 2011;**125**:145-179.
35. Serrano V, Liu W, Franzen S. An infrared spectroscopic study of the conformational transition of elastin-like polypeptides. *Biophys J* 2007;**93**:2429-2435.
36. Jeon WB. Application of elastin-mimetic recombinant proteins in chemotherapeutics delivery, cellular engineering, and regenerative medicine. *Bioengineered* 2013;**4**:368-373.
37. Bidwell III GL, Davis AN, Fokt I, Priebe W, Raucher D. A thermally targeted elastin-like polypeptide-doxorubicin conjugate overcomes drug resistance. *Invest New Drugs* 2007;**25**:313-326.
38. Bidwell III GL, Perkins E, Raucher D. A thermally targeted c-Myc inhibitory polypeptide inhibits breast tumor growth. *Cancer Lett* 2012;**319**:136-143.
39. Chen Y, Youn P, Furgeson DY. Thermo-targeted drug delivery of geldanamycin to hyperthermic tumor margins with diblock elastin-based biopolymers. *J Control Release* 2011;**155**:175-183.
40. Liu W, MacKay JA, Dreher MR, Chen M, McDaniel JR, Simnick AJ, et al. Injectable intratumoral depot of thermally responsive polypeptide-radionuclide conjugates delays tumor progression in a mouse model. *J Control Release* 2010;**144**:2-9.
41. Shamji MF, Chen J, Friedman AH, Richardson WJ, Chilkoti A, Setton LA. Synthesis and characterization of a thermally-responsive tumor necrosis factor antagonist. *J Control Release* 2008;**129**:179-186.
42. Simnick AJ, Amiram M, Liu W, Hanna G, Dewhirst MW, Kontos CD, et al. In vivo tumor targeting by a NGR-decorated micelle of a recombinant diblock copolypeptide. *J Control Release* 2011;**155**:144-151.
43. Sun G, Hsueh PY, Janib SM, Hamm-Alvarez S, MacKay JA. Design and cellular internalization of genetically engineered polypeptide nanoparticles displaying adenovirus knob domain. *J Control Release* 2011;**155**:218-226.
44. Wojcik-Stanaszek L, Gregor A, Zalewska T. Regulation of neurogenesis by extracellular matrix and integrins. *Acta Neurobiol Exp (Wars)* 2011;**71**:103-112.
45. Cox G, Crossley J, Xing Z. Macrophage engulfment of apoptotic neutrophils contributes to the resolution of acute pulmonary inflammation in vivo. *Am J Respir Cell Mol Biol* 1995;**12**:232-237.
46. Haslett C. Granulocyte apoptosis and its role in the resolution and control of lung inflammation. *Am J Respir Crit Care Med* 1999;**160**:S5-11.
47. Xue M, Del Bigio MR. Intracerebral injection of autologous whole blood in rats: time course of inflammation and cell death. *Neurosci Lett* 2000;**283**:230-232.
48. Zhao X, Sun G, Zhang J, Strong R, Song W, Gonzales N, et al. Hematoma resolution as a target for intracerebral hemorrhage treatment: role for peroxisome proliferator-activated receptor gamma in microglia/macrophages. *Ann Neurol* 2007;**61**:352-362.
49. Ruggeri ZM, Ware J. The structure and function of von Willebrand factor. *Thromb Haemost* 1992;**67**:594-599.
50. van der Sande JJ, Veltkamp JJ, Boekhout-Mussert RJ, Vielvoye GJ. Hemostasis and computerized tomography in head injury. Their relationship to clinical features. *J Neurosurg* 1981;**55**:718-724.

51. Yokota H, Naoe Y, Nakabayashi M, Unemoto K, Kushimoto S, Kurokawa A, et al. Cerebral endothelial injury in severe head injury: the significance of measurements of serum thrombomodulin and the von Willebrand factor. *J Neurotrauma* 2002;**19**:1007-1015.
52. Turaj W, Slowik A, Szczudlik A. Factors related to the occurrence of hyperthermia in patients with acute ischaemic stroke and with primary intracerebral haemorrhage. *Neurol Neurochir Pol* 2008;**42**:316-322.
53. Kasdorf E, Perlman JM. Hyperthermia, inflammation, and perinatal brain injury. *Pediatr Neurol* 2013;**49**:8-14.
54. Seri L, Rossiter JP, MacNair L, Flavin MP. Impact of hyperthermia on inflammation-related perinatal brain injury. *Dev Neurosci* 2012;**34**:525-532.